



Dynamic scanning probe microscopy of adsorbed molecules on graphite

N. Berdunov, A. J. Pollard, and P. H. Beton

Citation: *Applied Physics Letters* **94**, 043110 (2009); doi: 10.1063/1.3075054

View online: <http://dx.doi.org/10.1063/1.3075054>

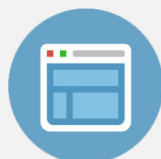
View Table of Contents: <http://scitation.aip.org/content/aip/journal/apl/94/4?ver=pdfcov>

Published by the [AIP Publishing](#)



Re-register for Table of Content Alerts

Create a profile.



Sign up today!



Dynamic scanning probe microscopy of adsorbed molecules on graphite

N. Berdunov,^{a)} A. J. Pollard, and P. H. Beton

School of Physics and Astronomy, University of Nottingham, Nottingham NG7 2RD, United Kingdom

(Received 5 August 2008; accepted 6 January 2009; published online 27 January 2009)

We have used a combined dynamic scanning tunneling and atomic force microscope to study the organization of weakly bound adsorbed molecules on a graphite substrate. These weakly bound molecules may be imaged in dynamic scanning tunneling microscopy (STM) mode in which the probe is oscillated above the surface. We show that molecular resolution may be readily attained and that a similar mode of imaging may be realized using conventional STM arrangement. We also show, using tunneling spectroscopy, the presence of an energy gap for the adsorbed molecules confirming a weak molecule-substrate interaction. © 2009 American Institute of Physics. [DOI: 10.1063/1.3075054]

Shortly after the invention of scanning probe microscopy, the imaging of adsorbed molecules emerged as a major theme of research, which has since grown to encompass manipulation and self-assembly phenomena and is also highly relevant to organic electronics.^{1–4} While the initial focus was on the use of scanning tunneling microscopy (STM) to acquire images with molecular resolution, there has recently been great progress in applying atomic force microscopy (AFM) to the imaging of adsorbed molecules.⁵ Images have now been acquired by a number of groups using either cantilevers or quartz tuning forks (TFs) as force sensors.^{6,7} Within this body of work the approach of Giessibl and co-workers^{8–10} is particularly attractive since it is well suited to the simultaneous measurement of tunnel currents and force gradients. In addition this approach has led to different imaging modes such as dynamic STM.¹⁰

In this paper we show that it is possible to resolve single molecules using dynamic STM and also demonstrate additional attractive features such as improved stability, as compared with conventional STM. We also show that these advantages may be realized using a conventional STM tip. For the molecule studied, perylene tetracarboxylic di-imide (PTCDI) adsorbed on graphite, we also observe a reproducible contrast inversion in the dynamic mode of STM.

The instrument we have constructed and used for our experiments is a scanning probe microscope based on TF force sensor,⁷ which is operated under ultrahigh vacuum (UHV) conditions at room temperature. The instrument can operate in three different regimes in conjunction with the TF sensor (spring constant $k=1800$ N/m): dynamic AFM in constant frequency mode (feedback signal: frequency shift); conventional (dc) STM in constant current mode (feedback signal: tip-sample current); and dynamic (ac) STM in constant average current mode (feedback signal: time averaged tip-sample current). For dynamic STM/AFM measurements the TF is mechanically excited using a small segment of the same piezotube used for x, y, z movement of the TF. For a metallic tip we use an electrochemically etched 25 μm diameter PtIr wire glued at the end of the TF and cleaned in UHV by Ar ion sputtering. After attachment of the tip the resonant frequency (measured in UHV) of the TF, f_0 , is in the range of 25–32 kHz with a Q -factor of 2000–5000. The

tip is electrically isolated from the TF electrodes and connected to the tunnel current preamplifier by a separate electrical connection. The bias voltage is applied to the sample.

Our experimental arrangement also permits the attachment of a conventional STM tip (we use cut PtIr wire), rather than the TF sensor, to the piezoelectric scanner. Dynamic STM is also possible in this configuration and can be realized by applying an sinusoidal signal to the piezoelectric scanner in order to induce an oscillatory motion of the tip (frequency of 29 kHz, amplitude of 0.2–0.3 nm) perpendicular to the surface (defined as the z direction). In all cases GXSM software¹¹ is used for control/data acquisition and WSXM for image processing.¹²

A highly oriented pyrolytic graphite (HOPG) sample was cleaved in air and transferred immediately into a UHV chamber. PTCDI was sublimed onto the HOPG substrate (held at room temperature) at an approximate deposition rate of 0.2 ML/min. Deposition of PTCDI results in the formation of highly faceted rodlike islands with typical widths of ~ 6 nm. These islands grow across step edges and form branched structures as imaged in the AFM mode of operation [Fig. 1(a)]. Second layer formation starts even for submonolayer coverage indicating a Volmer–Weber growth mode, which might be expected for a passive substrate such as graphite, and has also been observed in earlier reports of PTCDI growth on MoS₂.¹³ Interestingly, while there have been many studies of adsorbed molecules on graphite at a liquid/solid interface,¹⁴ there have been relatively few STM studies performed under vacuum conditions, and many of the published images were acquired at low temperature.^{15–17} One reason for this is the relatively weak adsorbate-graphite interaction, which results both in rapid diffusion of adsorbates and also gives rise to the potential for damage of any overlayers through interaction with the STM tip.

STM imaging (dc mode) of the PTCDI islands often results in island disruption presumably due to tip-molecule interactions (see above). Such tip-induced surface modification is demonstrated in Fig. 1(b) where the double-layer island is significantly disrupted following several consecutive scans using a tip mounted on a TF sensor in dc-STM mode. However, images of PTCDI islands can be readily acquired using dynamic STM. We reiterate that in this mode, a time averaged tunnel current between sample surface and oscillating tip is used to control probe height. Figure 1(e) shows a

^{a)}Electronic mail: nikolai.berdunov@nottingham.ac.uk.

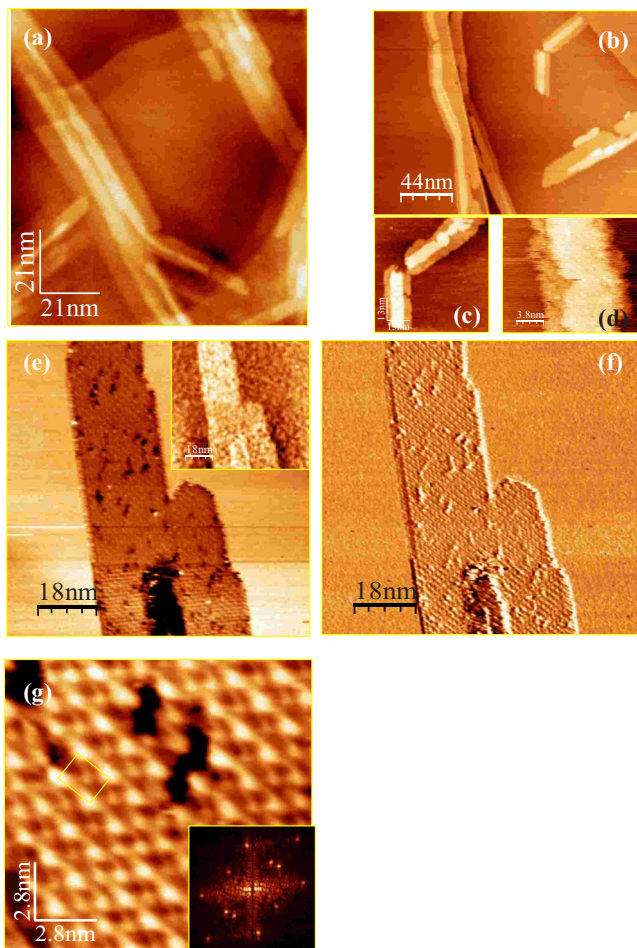


FIG. 1. (Color online) Images of PTCDI islands on HOPG surface acquired with TF sensor: (a) AFM topography ($df = -3$ Hz; $A_{osc} = 0.5$ nm). [(b)–(d)] dc-STM images showing islands grown on graphite. Regions of the needle-like growth shown in the top region of (b) are disrupted by successive scanning [see (c) and (d), which show removal of molecules from the island edge ($I_t = 80$ pA, $V_{bias} = 2.0$ V)]. (e) Dynamic STM image showing negative height contrast of ~ 0.1 nm per layer ($I_t = 30$ pA, $V_{bias} = -0.9$ V, $A_{osc} = 0.5$ nm). (Inset) Simultaneously acquired frequency shift (brighter features correspond to higher attractive forces). (f) ac component of the tunnel current recorded simultaneously with (e). (g) shows close-packed arrangement within the island (unit cell of 1.5×1.8 nm² is marked). (Inset) 2D Fourier image.

topographic image acquired in dynamic STM mode using a TF mounted tip. Unexpectedly, the PTCDI islands are imaged as a depression of approximately 0.1 nm, in contrast to a 0.14 nm protrusion in AFM and conventional STM measurements. Simultaneously with topographic dynamic STM imaging we acquire the frequency shift of the TF oscillation df and the oscillatory component, with frequency f_0 , of the tunnel current. Negative df values correspond to a positive force gradient. The df image in Fig. 1(e) inset shows an increase in the tip-surface attractive interaction when the tip is positioned on top of the PTCDI island, consistent with the topography image in Fig. 1(e). The a.c. component of the tunnel current [Fig. 1(f)] does not show a significant contrast variation between bare graphite and PTCDI.

A high resolution dynamic STM image in Fig. 1(g) reveals a close-packed arrangement of PTCDI with a unit cell of 1.5×1.8 nm². The elongated shape of the islands can be explained by anisotropy of intermolecular interactions, which arises from the interaction of imide and carbonyl groups on neighboring molecules as was previously observed for PTCDI and related molecules.^{18,19}

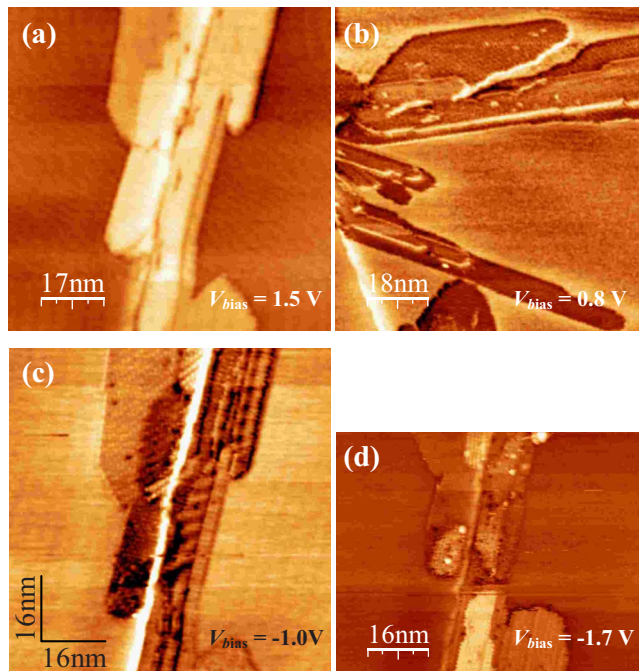


FIG. 2. (Color online) [(a)–(d)] Dynamic STM images of PTCDI islands acquired using a conventional STM tip ($I_t = 30$ pA, $A_{osc} = 0.2$ nm). Images acquired using sample biases (a) 1.8 V, (b) 0.8 V, (c) -1.0 V, and (d) -1.7 V to illustrate the bias dependence of the negative contrast of the PTCDI islands. (e) Tunneling spectroscopy acquired in dynamic STM mode above the graphite surface and over a PTCDI island illustrating the band gap of the adsorbed molecules.

To determine the origin of the negative contrast in Fig. 1, we have acquired a set of images of PTCDI islands using dynamic STM with a conventional (non-TF) tip for several different applied bias voltages. These images show that for large absolute bias voltages (1.5 and -1.7 V) a positive contrast is observed [Figs. 2(a) and 2(d), respectively], whereas for smaller absolute bias (0.8 and -1.0 V) negative contrast is observed similar to that observed in Fig. 1. For the lower absolute voltages it is not possible to acquire images in dc-STM. Also shown in Fig. 2 is an $I(V)$ curve acquired with the tip positioned (statically) over either the graphite or a PTCDI island. A tunneling gap is clearly present over the PTCDI island. A tunneling gap is clearly present over the PTCDI molecules, and this low tunnel current region accounts for the negative contrast that we observe. The large tunneling gap observed when the tip is placed above a molecule indicates that, as expected, the electronic coupling between molecule and surface is rather weak.

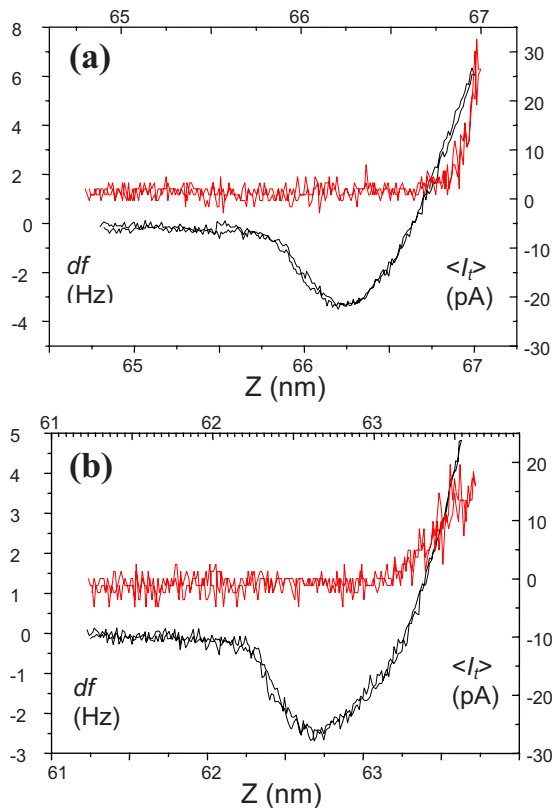


FIG. 3. (Color online) Frequency shift (black) and tunnel current (red/grey) vs distance measured using a TF sensor on (a) bare HOPG and (b) above a PTCDI island. Both approach and withdraw curves are shown. Horizontal axes are given in absolute Z position values.

To investigate further the contrast in dynamic STM we compare in Fig. 3 the variation in frequency shift (df) and average current ($\langle I_t \rangle$) with z , the tip position, acquired above either the bare graphite or a PTCDI island. There is noticeable broadening of the dependence of df on z (tip position) over a PTCDI island. In addition, the $\langle I_t \rangle$ versus z curve has a much less rapid rise as compared with the equivalent curve acquired on the bare HOPG surface.

To model the average current versus distance dependence we use the common approximation for tunnel current dependence on work function for conventional STM,²⁰ which leads for dynamic STM to the following expression for average tunnel current:

$$\begin{aligned} \langle I_t \rangle &= I_0 \int_0^{1/f_0} \exp\{-2a\varphi^{1/2}[z + A_{\text{osc}} \sin(2\pi f_0 t)]\} dt \\ &= I_0 \exp[-2a\varphi^{1/2}z] J_0(2aA_{\text{osc}}\varphi^{1/2}), \end{aligned} \quad (2)$$

where J_0 is the modified Bessel function of the first kind, A_{osc} is the amplitude of the tip oscillation, φ is the work function, and $a = (2m)^{1/2}/\hbar$. The exponential dependence of $\langle I_t \rangle$ on z is consistent with our experimental measurements (Fig. 3).

Overall our results show that in regions where contrast inversion occurs, which might be expected for weakly bound molecules, image acquisition using conventional dc-STM is difficult, if not impossible, but images can be acquired with molecular resolution using dynamic STM. We argue that the reason for the enhanced imaging stability is the oscillatory motion of the STM tip, which means that when in close

proximity to the molecules, the tip is moving perpendicular to the surface. A consequence of this is that as the tip passes over the molecular islands (including the edges), the lateral forces that are generated between tip and molecule are expected to be much lower than those that occur for conventional imaging [and are well known to lead to molecular displacement across surfaces (see, for example, Ref. 21)]. The relative stability of dynamic STM may be considered analogous to the enhanced stability of tapping mode, as compared with contact-mode AFM. The curves shown in Fig. 3 support the presence of significant tip-molecule forces through the broadening of the minimum of the force-gradient versus height curve.

In conclusion, we have demonstrated that dynamic STM may be used to acquire structural and electronic measurements for molecular assemblies weakly bound to a substrate. For the case of PTCDI nanosized islands on a graphite surface, the stability and resolution that may be attained in dynamic STM is significantly better than under dc-STM. Furthermore, we demonstrate that dynamic STM may be realized in a conventional (non-TF) STM and that this imaging technique therefore has the potential to be applied to a wide range of materials where stable image acquisition is not possible using dc-STM.

This work was supported by the UK Engineering and Physical Sciences Research Council under Grant No. GR/C534158/1. We are very grateful to R. J. Chettle and D. J. Laird for technical support and we thank N. R. Champness, P. Moriarty, and C. J. Mellor for helpful discussions.

- ¹C. Joachim, J. K. Gimzewski, and A. Aviram, *Nature (London)* **408**, 541 (2000).
- ²J. V. Barth, G. Costantini, and K. Kern, *Nature (London)* **437**, 671 (2005).
- ³S. R. Forrest, *Nature (London)* **428**, 911 (2004).
- ⁴F. Rosei, M. Schunack, Y. Naitoh, P. Jiang, A. Gourdon, E. Laegsgaard, I. Stensgaard, C. Joachim, and F. Besenbacher, *Prog. Surf. Sci.* **71**, 95 (2003).
- ⁵K. Kobayashi, H. Yamada, T. Horiuchi, and K. Matsushige, *Appl. Surf. Sci.* **157**, 228 (2000).
- ⁶R. Garcia and R. Perez, *Surf. Sci. Rep.* **47**, 197 (2002).
- ⁷F. J. Giessibl, *Science* **267**, 68 (1995).
- ⁸A. Mayer, *Appl. Phys. Lett.* **86**, 153110 (2005).
- ⁹S. Hembacher, F. J. Giessibl, and J. Mannhart, *Phys. Rev. Lett.* **94**, 056101 (2005).
- ¹⁰L. A. Zotti, W. A. Hofer, and F. J. Giessibl, *Chem. Phys. Lett.* **420**, 177 (2006).
- ¹¹P. Zahl, M. Bierkandt, S. Schröder, and A. Klust, *Rev. Sci. Instrum.* **74**, 1222 (2003).
- ¹²I. Horcas, R. Fernandez, J. M. Gomez-Rodriguez, J. Colchero, J. Gomez-Herrero, and A. M. Baro, *Rev. Sci. Instrum.* **78**, 013705 (2007).
- ¹³C. Ludwig, B. Gompf, J. Petrsen, R. Strohmaier, and W. Eisenmenger, *Z. Phys. B: Condens. Matter* **93**, 365 (1994).
- ¹⁴S. De Feyter and F. C. De Schryver, *Chem. Soc. Rev.* **32**, 139 (2003).
- ¹⁵S. Griessl, M. Lackinger, M. Edelwirth, M. Hietschold, and W. M. Heckl, *Single Mol.* **3**, 25 (2002).
- ¹⁶T. G. Gopakumar, J. Meiss, D. Pouladsaz, and M. Hietschold, *J. Phys. Chem. C* **112**, 2529 (2008).
- ¹⁷L. Kleiner-Shuhler, R. Brittain, M. R. Johnston, and K. W. Hipps, *J. Phys. Chem. C* **112**, 14907 (2008).
- ¹⁸J. C. Swarbrick, J. Ma, J. A. Theobald, N. S. Oxtoby, J. N. O'Shea, N. R. Champness, and P. H. Beton, *J. Phys. Chem. B* **109**, 12167 (2005).
- ¹⁹D. L. Keeling, N. S. Oxtoby, C. Wilson, M. J. Humphry, N. R. Champness, and P. H. Beton, *Nano Lett.* **3**, 9 (2003).
- ²⁰G. Binnig, H. Rohrer, C. Gerber, and E. Weibel, *Appl. Phys. Lett.* **40**, 178 (1982).
- ²¹D. L. Keeling, M. J. Humphry, P. Moriarty, and P. H. Beton, *Chem. Phys. Lett.* **366**, 300 (2002).